

Fluctuation-Dissipation Theorem in an Isolated System of Quantum Dipolar Bosons after a Quench

Ehsan Khatami,¹ Guido Pupillo,² Mark Srednicki,³ and Marcos Rigol⁴

¹*Department of Physics, University of California, Santa Cruz, California 95064, USA*

²*IPCMS (UMR 7504) and ISIS (UMR 7006), Université de Strasbourg and CNRS, Strasbourg, France*

³*Department of Physics, University of California, Santa Barbara, California 93106, USA*

⁴*Department of Physics, The Pennsylvania State University, University Park, Pennsylvania 16802, USA*

We examine the validity of fluctuation-dissipation relations in isolated quantum systems taken out of equilibrium by a sudden quench. We focus on the dynamics of trapped hard-core bosons in one-dimensional lattices with dipolar interactions whose strength is changed during the quench. We find indications that fluctuation-dissipation relations hold if the system is nonintegrable after the quench, as well as if it is integrable after the quench if the initial state is an equilibrium state of a nonintegrable Hamiltonian. On the other hand, we find indications that they fail if the system is integrable both before and after quenching.

PACS numbers: 05.30.Jp, 03.75.Kk, 05.40.-a, 67.85.-d

The fluctuation-dissipation theorem (FDT) [1–3] is a fundamental relation in statistical mechanics which states that typical deviations from the equilibrium state caused by an external perturbation (within the linear response regime) dissipate in time in the same way as random fluctuations. The theorem applies to both classical and quantum systems as long as they are in thermal equilibrium. Fluctuation-dissipation relations are not, in general, satisfied for out-of-equilibrium systems. In particular, if a system is isolated, it is not clear whether once taken far from equilibrium fluctuation-dissipation relations apply at any later time. Studies of integrable models such as a Luttinger liquid [4] and the transverse field Ising chain [5] have shown that the use of fluctuation-dissipation relations to define temperature leads to values of the temperature that depend on the momentum mode and/or the frequency being considered. More recently, Essler *et al.* [6] have shown that for a subsystem of an isolated infinite system, the basic form of the FDT holds, and that the same ensemble that describes the static properties also describes the dynamics.

The question of the applicability of the FDT to isolated quantum systems is particularly relevant to experiments with cold atomic gases [7, 8], whose dynamics is considered to be, to a good approximation, unitary [9]. In that context, the description of observables after relaxation (whenever relaxation to a time-independent value occurs) has been intensively explored in the recent literature [10]. This is because, for isolated quantum systems out of equilibrium, it is not apparent that thermalization can take place. For example, if the system is prepared in an initial pure state $|\phi_{\text{ini}}\rangle$ that is not an eigenstate of the Hamiltonian \hat{H} ($\hat{H}|\psi_\alpha\rangle = E_\alpha|\psi_\alpha\rangle$) (as in Ref. [9]), then the infinite-time average of the evolution of the observable \hat{O} can be written as $\langle \hat{O}(t) \rangle = \sum_\alpha |c_\alpha|^2 O_{\alpha\alpha} \equiv O_{\text{diag}}$, where $c_\alpha = \langle \psi_\alpha | \phi_{\text{ini}} \rangle$, $O_{\alpha\alpha} = \langle \psi_\alpha | \hat{O} | \psi_\alpha \rangle$, and we have assumed that the spectrum is nondegenerate. The outcome of the infinite-time average can be thought of as the prediction of a “diagonal” ensemble [11]. O_{diag} depends on the initial state through the c_α 's (there is an exponentially large number of them), while the thermal predictions depend only on the total energy $\langle \phi_{\text{ini}} | \hat{H} | \phi_{\text{ini}} \rangle$; i.e., they need not agree.

The lack of thermalization of some observables, in the spe-

cific case of quasi-one-dimensional geometries close to an integrable point, was seen in experiments [12] short-range and, at integrability, confirmed in computational [13] and analytical [14] calculations. Away from integrability, computational studies have shown that few-body observables thermalize in general [11, 15–17], which can be understood in terms of the eigenstate thermalization hypothesis (ETH) [11, 18, 19]. We note that the nonintegrable systems studied computationally belong to two main classes of lattice models: (i) spin-polarized fermions, hard-core bosons, and spin models with short-range (nearest and next-nearest-neighbor) interactions [11, 15, 16, 20] and (ii) the Bose-Hubbard model [17].

In this Letter, we go beyond these studies and report results that indicate that fluctuation-dissipation relations are also valid in generic isolated quantum systems after relaxation, while they fail at integrability. For that, we use exact diagonalization and study a third class of lattice models, hard-core bosons with dipolar interactions in one dimension [21]. The latter are of special interest as they describe experiments with quantum gases of magnetic atoms trapped in optical lattices [22] as well as ground state polar molecules [23]. Rydberg-excited alkali atoms [24] and laser-cooled ions [25] may soon provide alternative realizations of correlated systems with dipolar interactions. The effect of having power-law decaying interactions in the dynamics and description of isolated quantum systems after relaxation is an important and open question that we address here.

The model Hamiltonian for those systems can be written as

$$\hat{H} = -J \sum_{j=1}^{L-1} \left(\hat{b}_j^\dagger \hat{b}_{j+1} + \text{H.c.} \right) + V \sum_{j < l} \frac{\hat{n}_j \hat{n}_l}{|j-l|^3} + g \sum_j x_j^2 \hat{n}_j \quad (1)$$

where \hat{b}_j^\dagger (\hat{b}_j) creates (annihilates) a hard-core boson ($\hat{b}_j^{\dagger 2} = \hat{b}_j^2 = 0$) at site j , and $\hat{n}_j = \hat{b}_j^\dagger \hat{b}_j$ is the number operator. J is the hopping amplitude, V the strength of the dipolar interaction, g the strength of the confining potential, x_j the distance of site j from the center of the trap, and L the number of lattice sites (the total number of bosons p is always chosen to be $p = L/3$). We set $J = 1$ (unit of energy throughout this paper), $\hbar = k_B = 1$, use open boundary conditions, and work in the

subspace with even parity under reflection.

We focus on testing a fluctuation-dissipation relation after a quench for experimentally relevant observables, namely, site and momentum occupations (results for the density-density structure factor are presented in Ref. [26]). A scenario under which FDT holds in isolated systems out of equilibrium was put forward by one of us in Ref. [27]. There, it was shown that after a quantum or thermal fluctuation (assumed to occur at time t' [28], which was treated as a uniformly distributed random variable), it is overwhelmingly likely that $O_{t' \pm t} = C_{\text{Fluc}}(t)O_{t'}$, where $O_t = \langle \hat{O}(t) \rangle$ [29]. Formally, $C_{\text{Fluc}}(t)$ is related to the second moments of a probability distribution for O_t , $C_{\text{Fluc}}(t) = \overline{O_{t+t''}O_{t''}} / (\overline{O_{t''}})^2$, where infinite-time averages have been taken with respect to t'' . Therefore, assuming that no degeneracies occur in the many-body spectrum or that they are unimportant, $C_{\text{Fluc}}(t)$ can be written as

$$C_{\text{Fluc}}(t) \propto \sum_{\substack{\alpha\beta \\ \alpha \neq \beta}} |c_\alpha|^2 |c_\beta|^2 |O_{\alpha\beta}|^2 e^{i(E_\alpha - E_\beta)t}, \quad (2)$$

where the proportionality constant is such that $C_{\text{Fluc}}(0) = 1$ [30]. The correlation function in Eq. (2) explicitly depends on the initial state through c_α .

Assuming that eigenstate thermalization occurs in the Hamiltonian of interest, the matrix elements of \hat{O} in the energy eigenstate basis can be written as

$$O_{\alpha\beta} = \Omega(E)\delta_{\alpha\beta} + e^{-S(E)/2} f(E, \omega) R_{\alpha\beta}, \quad (3)$$

where $E \equiv \frac{1}{2}(E_\alpha + E_\beta)$, $\omega \equiv E_\alpha - E_\beta$, $S(E)$ is the thermodynamic entropy at energy E , $e^{S(E)} = E \sum_\alpha \delta(E - E_\alpha)$, $\Omega(E)$ and $f(E, \omega)$ are smooth functions of their arguments, and $R_{\alpha\beta}$ is a random variable (e.g., with zero mean and unit variance). This is consistent with quantum chaos theory and is presumably valid for a wide range of circumstances [27, 31]. From Eq. (3), it follows straightforwardly that $C_{\text{Fluc}}(t) \sim C_{\text{Appr}}(t)$, where we have defined

$$C_{\text{Appr}}(t) \propto \int_{-\infty}^{+\infty} d\omega |f(E, \omega)|^2 e^{i\omega t}, \quad (4)$$

and again, the proportionality constant is such that $C_{\text{Appr}}(0) = 1$ [32]. Therefore, we see that $C_{\text{Fluc}}(t)$ does not depend on the details of the initial state, in the same way that observables in the diagonal ensemble do not depend on such details.

We can then compare this result to how a typical deviation from thermal equilibrium (used to describe observables in the nonequilibrium system after relaxation) caused by an external perturbation ‘‘dissipates’’ in time. Assuming that the perturbation is small (linear response regime) and that it is applied at time $t = 0$, $C_{\text{Diss}}(t)$, defined via $O_t = C_{\text{Diss}}(t)O_{\text{Thermal}}$, can be calculated through Kubo’s formula as [27, 33]

$$C_{\text{Diss}}(t) \propto \sum_{\substack{\alpha\beta \\ \alpha \neq \beta}} \frac{e^{-E_\alpha/T} - e^{-E_\beta/T}}{E_\beta - E_\alpha} |O_{\alpha\beta}|^2 e^{i(E_\alpha - E_\beta)t}, \quad (5)$$

where again, we set $C_{\text{Diss}}(0) = 1$. Using Eq. (3), one finds that

$$C_{\text{Diss}}(t) \sim \int_{-\infty}^{+\infty} d\omega \frac{\sinh(\omega/2T)}{\omega} |f(E, \omega)|^2 e^{i\omega t} \sim C_{\text{Appr}}(t), \quad (6)$$

where the last similarity is valid if the width of $f(E, \omega)$ [26] is of the order of, or smaller than, the temperature. The results in Eqs. (4) and (6) suggest that FDT holds in isolated quantum systems out of equilibrium under very general conditions.

In what follows, we study dipolar systems out of equilibrium and test whether their dynamics is consistent with the scenario above. This is a first step toward understanding the relevance of FDT and of the specific scenario proposed in Ref. [27], to experiments with nonequilibrium ultracold quantum gases. The dynamics are studied after sudden quenches, for which the initial pure state $|\phi_{\text{ini}}\rangle$ is selected to be an eigenstate of Eq. (1) for $V = V_{\text{ini}}$ and $g = g_{\text{ini}}$ (\hat{H}_{ini}), and the evolution is studied under \hat{H}_{fin} ($V = V_{\text{fin}}$ and $g = g_{\text{fin}}$), i. e., $|\phi(t)\rangle = e^{-i\hat{H}_{\text{fin}}t} |\phi_{\text{ini}}\rangle$. We consider the following three types of quenches: type (i) $\{V_{\text{ini}} = 0, g_{\text{ini}} = \gamma\} \rightarrow \{V_{\text{fin}} = 0, g_{\text{fin}} = \gamma/10\}$ (integrable to integrable), type (ii) $\{V_{\text{ini}} = 8, g_{\text{ini}} = \gamma\} \rightarrow \{V_{\text{fin}} = 0, g_{\text{fin}} = \gamma\}$ (nonintegrable to integrable), and type (iii) $\{V_{\text{ini}} = 8, g_{\text{ini}} = \gamma\} \rightarrow \{V_{\text{fin}} = 2, g_{\text{fin}} = \gamma\}$ (nonintegrable to nonintegrable). We choose γ such that $\gamma x_1^2 = \gamma x_L^2 = 4$, which ensures a (nearly) vanishing density at the edges of the lattice in the ground state. The initial state for different quenches, which need not be the ground state of \hat{H}_{ini} , is selected such that $E_{\text{tot}} = \langle \phi_{\text{ini}} | \hat{H}_{\text{fin}} | \phi_{\text{ini}} \rangle$ corresponds to the energy of a canonical ensemble with temperature $T = 5$, i. e., such that $E_{\text{tot}} = \text{Tr}\{e^{-\hat{H}_{\text{fin}}/T} \hat{H}_{\text{fin}}\} / \text{Tr}\{e^{-\hat{H}_{\text{fin}}/T}\}$.

In Fig. 1, we show results for $C_{\text{Fluc}}(t)$, $C_{\text{Diss}}(t)$, and $C_{\text{Appr}}(t)$ when the observable of interest is the occupation of the site in the center of the system $n_{j=L/2}$ (qualitatively similar results were obtained for other site occupations, for momenta occupations, and for the density-density structure factor [26]). The results are obtained for the three different quench types mentioned above and are shown for $L = 15$ and 18. For quench type (i), we find that none of the three correlation functions agree with each other and that the agreement does not improve with increasing L [see Figs. 1(a) and 1(b)]. There are also large time fluctuations, characteristic of the integrable nature of the final Hamiltonian [34]. We quantify these fluctuations by plotting the histograms of $C_{\text{Fluc}}(t)$ and $C_{\text{Diss}}(t)$ for an extended period of time in the insets. We find the histograms to be broad functions for quenches (i) and (ii) [Figs. 1(a)-1(d)].

Remarkably, in quenches type (ii) [Figs. 1(c) and 1(d)], which also have a final Hamiltonian that is integrable, $C_{\text{Fluc}}(t)$ and $C_{\text{Diss}}(t)$ are very similar to each other at each time and their differences decrease with increasing L . This indicates that the FDT holds. At the same time, we find differences between fluctuation or dissipation correlations and $C_{\text{Appr}}(t)$, indicating that the agreement between $C_{\text{Fluc}}(t)$ and $C_{\text{Diss}}(t)$ does not imply that Eq. (3) is valid. These observations can be understood if the initial state provides an unbiased sampling of the eigenstates of the final Hamiltonian. In that case, even though eigenstate thermalization does not occur, thermaliza-

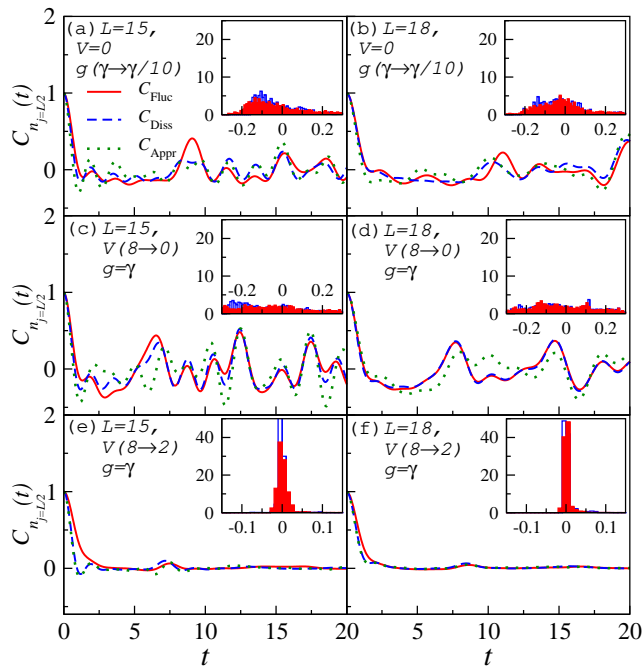


FIG. 1. Correlation functions $C_{\text{Fluc}}(t)$, $C_{\text{Diss}}(t)$, and $C_{\text{Appr}}(t)$ when the observable is $n_{j=L/2}$ vs time t . Results are shown for the three quenches (i)-(iii) (from top to bottom, respectively) explained in the text, and for $L = 15$ (left panels) and 18 (right panels). Results for $L = 12$ are presented in Ref. [26]. The insets show normalized histograms of $C_{\text{Fluc}}(t)$ (filled red bars) and $C_{\text{Diss}}(t)$ (empty blue bars) calculated for 2000 data points between $t = 0$ and 100 .

tion can take place [35], and this results in the applicability of FDT. In quenches type (ii), such an unbiased sampling occurs because of the nonintegrability of the initial Hamiltonian, whose eigenstates are random superpositions of eigenstates of the final integrable Hamiltonian with close energies [35].

For quenches type (iii) [Figs. 1(e) and 1(f)], on the other hand, we find that not only $C_{\text{Fluc}}(t)$ and $C_{\text{Diss}}(t)$ are very close to each other, but also $C_{\text{Appr}}(t)$ is very close to both of them, and that the differences between the three decrease with increasing L . Therefore, our results are consistent with the system exhibiting eigenstate thermalization [36], which means that the assumptions made in Eq. (3) are valid, and the applicability of the FDT follows. Furthermore, for quenches type (iii), one can see that time fluctuations are strongly suppressed when compared to those in quenches type (i) and (ii) [better seen in the insets of Fig. 1(e) and 1(f)], which is a result of the nonintegrable nature of the final Hamiltonian [27, 37].

To quantify the differences between the three correlation functions and explore their dependence on the system size for each quench type, we calculate the normalized variances of $C_{\text{Fluc}}(t) - C_{\text{Diss}}(t)$ and $C_{\text{Fluc}}(t) - C_{\text{Appr}}(t)$. In Fig. 2, we show these quantities for the three quench types vs L . For quench type (i), the variances exhibit a tendency to saturate to a nonzero value as L increases, which indicates that $C_{\text{Fluc}}(t)$ and $C_{\text{Diss}}(t)$, as well as $C_{\text{Fluc}}(t)$ and $C_{\text{Appr}}(t)$, may remain different in the thermodynamic limit. This is consistent with

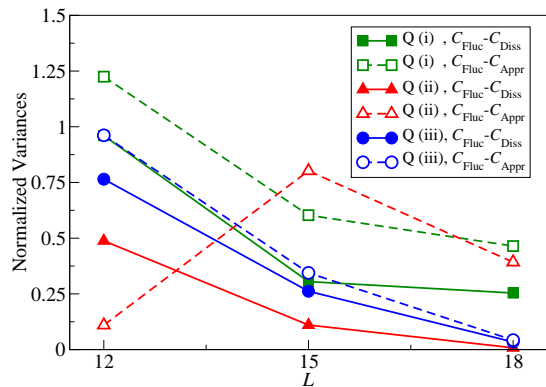


FIG. 2. Normalized variance of $C_{\text{Fluc}}(t) - C_{\text{Diss}}(t)$ and $C_{\text{Fluc}}(t) - C_{\text{Appr}}(t)$ vs the system size for the three quenches explained in the text [identified by Q (i), Q (ii), and Q (iii)], where the normalization factor is the average variance of the two functions for which the differences are calculated, e.g., $\text{Var}(C_{\text{Fluc}} - C_{\text{Diss}}) / \frac{1}{2}[\text{Var}(C_{\text{Fluc}}) + \text{Var}(C_{\text{Diss}})]$. The observable is $n_{j=L/2}$. The variances are calculated for 2000 points between $t = 0$ and 100 .

the findings in Refs. [4, 5], where it was shown that in the thermodynamic limit, conventional fluctuation-dissipation relations with a unique temperature do not hold in integrable systems. For quench type (ii), we see that the variance of $C_{\text{Fluc}}(t) - C_{\text{Diss}}(t)$ decreases with increasing system size and becomes very small already for $L = 18$, indicating that $C_{\text{Fluc}}(t)$ and $C_{\text{Diss}}(t)$ possibly agree in the thermodynamic limit. The variance of $C_{\text{Fluc}}(t) - C_{\text{Appr}}(t)$, on the other hand, exhibits a more erratic behavior, and it is not apparent whether it vanishes for larger system sizes. For quench type (iii), the relative differences between $C_{\text{Fluc}}(t)$, $C_{\text{Diss}}(t)$, and $C_{\text{Appr}}(t)$ exhibit a fast decline with increasing L , indicating that all three likely agree in the thermodynamic limit. These results strongly suggest that the FDT is applicable in the thermodynamic limit for quenches in which the final system is nonintegrable, as well as after quenches from nonintegrable to integrable systems, even though the ETH does not hold in the latter.

In order to gain an understanding of why FDT fails or applies depending on the nature of the final Hamiltonian, we explore to which extent Eq. (3) describes the behavior of the matrix elements of few-body observables in the nonintegrable case and in which way it breaks down at integrability. In Fig. 3, we plot the off-diagonal elements of two observables $n_{j=L/2}$ and the zero-momentum occupation number $n_{k=0}$ vs the eigenenergy differences (ω) in a narrow energy window around $E = E_{\text{tot}}$. Results are shown for matrix elements in the eigenstates of the final Hamiltonians in quenches type (ii) and (iii) [38]. The off-diagonal matrix elements of both observables in the eigenstates of the integrable Hamiltonian [Figs. 3(a) and 3(b)] exhibit a qualitatively different behavior from those in the nonintegrable one. In the integrable Hamiltonian, they exhibit extremely large fluctuations. In addition, a very large fraction of those elements (larger for $n_{j=L/2}$ than for $n_{k=0}$) have vanishing values. This makes any definition of a smooth function $f(E, \omega)$ meaningless. Those results contrast

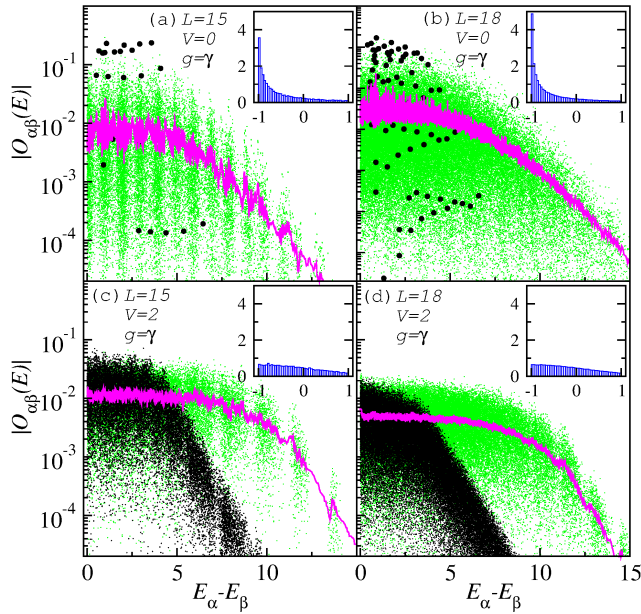


FIG. 3. Absolute value of the off-diagonal matrix elements of $\hat{n}_{j=L/2}$ and $\hat{n}_{k=0}$ in the eigenenergy basis, in a narrow energy window around $E = E_{\text{tot}}$ (with a width of 0.1) vs the eigenenergy difference $\omega = E_{\alpha} - E_{\beta}$. Results are shown for $L = 15$ (left panels) and $L = 18$ (right panels). (a),(b) and (c),(d) correspond to the final Hamiltonian in quenches (ii) and (iii), respectively. The green (light gray) symbols are the matrix elements of $\hat{n}_{k=0}$, and the black ones of $\hat{n}_{j=L/2}$. In (a) and (b), we have increased the size of the symbols for $n_{j=L/2}$ by a factor of 20 relative to those for $n_{k=0}$. To increase the resolution of the distribution of values in the case of $L = 18$, where a very large number of data points exists, we plot only 1 out of every 10 points for $n_{k=0}$ in (b) and for both observables in (d). Lines are running averages for $n_{k=0}$ with a subset length of 50 for $L = 15$ and 200 for $L = 18$. Insets show the histograms of the relative differences between the $n_{k=0}$ data and running averages (f_{avg}) with subset sizes of 1000 for $L = 15$ and 10 000 for $L = 18$. The relative difference is defined as $(|O_{\alpha\beta}| - f_{\text{avg}})/f_{\text{avg}}$.

the ones obtained in the nonintegrable case, where the fluctuations of the matrix elements have a different nature, and we do not find a large fraction of vanishing ones. To see that more clearly for $n_{k=0}$ (the better behaved of the two observables), in the insets of Fig. 3, we show the normalized histograms of the relative differences between the matrix elements for $n_{k=0}$ and a “smooth” function, defined as the running average of those elements over a large enough group of them (examples of the running averages are presented in the main panels). For the integrable system, we find that the histograms are not compatible with the uniform distribution postulated in Eq. (3), as a very sharp peak develops at -1 for both system sizes. That peak becomes sharper with increasing system size, reflecting an increasing fraction of vanishing off-diagonal matrix elements in those systems. For the nonintegrable Hamiltonian, on the other hand, the histograms are closer to a uniform distribution.

In summary, studying the dynamics of an experimentally relevant model of trapped hard-core bosons with dipolar in-

teractions, we have found indications that the FDT is applicable to the properties of few-body observables in nonintegrable isolated quantum systems out of equilibrium, and that this follows from the ETH. Furthermore, we find indications that the FDT may also apply to integrable systems, for which the ETH is not valid, provided that the initial state before the quench is an equilibrium state (eigenstate) of a nonintegrable system.

We acknowledge support from the National Science Foundation, under Grants No. OCI-0904597 (E.K. and M.R.) and No. PHY07-57035 (M.S.), and from the European Commission, under ERC-St Grant No. 307688 COLDSIM, UdS, and EOARD (G.P.). We are grateful to Aditi Mitra for motivating discussions.

-
- [1] H. Nyquist, Phys. Rev. **32**, 110 (1928).
 - [2] L. Onsager, Phys. Rev. **37**, 405 (1931).
 - [3] H. B. Callen and T. A. Welton, Phys. Rev. **83**, 34 (1951).
 - [4] A. Mitra and T. Giamarchi, Phys. Rev. Lett. **107**, 150602 (2011); Phys. Rev. B **85**, 075117 (2012).
 - [5] L. Foini, L. F. Cugliandolo, and A. Gambassi, Phys. Rev. B **84**, 212404 (2011); J. Stat. Mech. **09**, P09011 (2012).
 - [6] F. H. L. Essler, S. Evangelisti, and M. Fagotti, Phys. Rev. Lett. **109**, 247206 (2012).
 - [7] I. Bloch, J. Dalibard, and W. Zwerger, Rev. Mod. Phys. **80**, 885 (2008).
 - [8] M. A. Cazalilla, R. Citro, T. Giamarchi, E. Orignac, and M. Rigol, Rev. Mod. Phys. **83**, 1405 (2011).
 - [9] S. Trotzky, Y.-A. Chen, A. Flesch, I. P. McCulloch, U. Schollwöck, J. Eisert, and I. Bloch, Nat. Phys. **8**, 325 (2012).
 - [10] M. A. Cazalilla and M. Rigol, New J. Phys. **12**, 055006 (2010); J. Dziarmaga, Adv. Phys. **59**, 1063 (2010); A. Polkovnikov, K. Sengupta, A. Silva, and M. Vengalattore, Rev. Mod. Phys. **83**, 863 (2011).
 - [11] M. Rigol, V. Dunjko, and M. Olshanii, Nature (London) **452**, 854 (2008).
 - [12] T. Kinoshita, T. Wenger, and D. S. Weiss, Nature (London) **440**, 900 (2006); M. Gring, M. Kuhnert, T. Langen, T. Kitagawa, B. Rauer, M. Schreitl, I. Mazets, D. A. Smith, E. Demler, and J. Schmiedmayer, Science **337**, 1318 (2012).
 - [13] M. Rigol, V. Dunjko, V. Yurovsky, and M. Olshanii, Phys. Rev. Lett. **98**, 050405 (2007); M. Rigol, A. Muramatsu, and M. Olshanii, Phys. Rev. A **74**, 053616 (2006); A. C. Cassidy, C. W. Clark, and M. Rigol, Phys. Rev. Lett. **106**, 140405 (2011); D. Rossini, A. Silva, G. Mussardo, and G. E. Santoro, Phys. Rev. Lett. **102**, 127204 (2009); D. Rossini, S. Suzuki, G. Mussardo, G. E. Santoro, and A. Silva, Phys. Rev. B **82**, 144302 (2010).
 - [14] M. A. Cazalilla, Phys. Rev. Lett. **97**, 156403 (2006); P. Calabrese and J. Cardy, J. Stat. Mech. **06** P06008 (2007); M. Kollar and M. Eckstein, Phys. Rev. A **78**, 013626 (2008); A. Iucci and M. A. Cazalilla, Phys. Rev. A **80**, 063619 (2009); D. Fioretto and G. Mussardo, New J. Phys. **12**, 055015 (2010); P. Calabrese, F. H. L. Essler, and M. Fagotti, Phys. Rev. Lett. **106**, 227203 (2011); M. A. Cazalilla, A. Iucci, and M.-C. Chung, Phys. Rev. E **85**, 011133 (2012); P. Calabrese, F. H. L. Essler, and M. Fagotti, J. Stat. Mech. **07**, P07022 (2012).
 - [15] M. Rigol, Phys. Rev. Lett. **103**, 100403 (2009); Phys. Rev. A **80**, 053607 (2009); L. F. Santos and M. Rigol, Phys. Rev. E **81**, 036206 (2010); *ibid* **82**, 031130 (2010).

- [16] M. C. Bañuls, J. I. Cirac, and M. B. Hastings, Phys. Rev. Lett. **106**, 050405 (2011); C. Neuenhahn and F. Marquardt, Phys. Rev. E **85**, 060101 (2012).
- [17] C. Kollath, A. M. Läuchli, and E. Altman, Phys. Rev. Lett. **98**, 180601 (2007); G. Roux, Phys. Rev. A **79**, 021608 (2009); G. Roux, Phys. Rev. A **81**, 053604 (2010); G. Biroli, C. Kollath, and A. M. Läuchli, Phys. Rev. Lett. **105**, 250401 (2010).
- [18] J. M. Deutsch, Phys. Rev. A **43**, 2046 (1991).
- [19] M. Srednicki, Phys. Rev. E **50**, 888 (1994).
- [20] S. R. Manmana, S. Wessel, R. M. Noack, and A. Muramatsu, Phys. Rev. Lett. **98**, 210405 (2007).
- [21] T. Lahaye, C. Menotti, L. Santos, M. Lewenstein, and T. Pfau, Rep. Prog. Phys. **72**, 126401 (2007); M. A. Baranov, M. Dalmonte, G. Pupillo, and P. Zoller, Chem. Rev. **112**, 5012 (2012).
- [22] J. Billy, E. A. L. Henn, S. Müller, T. Maier, H. Kadau, A. Griesmaier, M. Jona-Lasinio, L. Santos, and T. Pfau, Phys. Rev. A **86**, 051603(R) (2012); B. Pasquiou, E. Maréchal, L. Vernac, O. Gorceix, and B. Laburthe-Tolra, Phys. Rev. Lett. **108**, 045307 (2012); K. Aikawa, A. Frisch, M. Mark, S. Baier, A. Rietzler, R. Grimm, and F. Ferlaino, Phys. Rev. Lett. **108**, 210401 (2012); M. Lu, N. Q. Burdick, and B. L. Lev, Phys. Rev. Lett. **108**, 215301 (2012).
- [23] D. Jin and J. Ye, Chem. Rev. **112**, 4081 (2012); L. Carr, D. DeMille, R. Krems, and J. Ye, New J. Phys. **11**, 055049 (2009); A. Chotia, B. Neyenhuis, S. A. Moses, B. Yan, J. P. Covey, M. Foss-Feig, A. M. Rey, D. S. Jin, and J. Ye, Phys. Rev. Lett. **108**, 080405 (2012); T. Takekoshi, M. Debatin, R. Rameshan, F. Ferlaino, R. Grimm, H.-C. Nägerl, C. R. L. Sueur, J. M. Hutson, P. S. Julienne, S. Kotochigova, et al., Phys. Rev. A **85**, 032506 (2012).
- [24] M. Saffman, T. G. Walker, and K. Mølmer, Rev. Mod. Phys. **82**, 2313 (2010); D. Comparat and P. Pillet, J. Opt. Soc. Am. B **27**, 208 (2010).
- [25] F. Mintert and C. Wunderlich, Phys. Rev. Lett. **87**, 257904 (2001); D. Porras and J. I. Cirac, Phys. Rev. Lett. **92**, 207901 (2004); R. Islam, C. Senko, W. C. Campbell, S. Korenblit, J. Smith, A. Lee, E. E. Edwards, C.-C. J. Wang, J. K. Freericks, and C. Monroe, arXiv:1210.0142; M. van den Worm, B. C. Sawyer, J. J. Bollinger, and M. Kastner, arXiv:1209.3697; C. Schneider, D. Porras, and T. Schätz, Rep. Prog. Phys. **75**, 024401 (2012).
- [26] See the Supplementary Materials.
- [27] M. Srednicki, J. Phys. A **32**, 1163 (1999).
- [28] Note that t' is not the time after the quench. The question of interest here is whether fluctuation-dissipation relations hold after the observable of interest has equilibrated following a sudden quench. We note that most of the time after the quench, the observable will be close to its infinite-time average (or equilibrated) value [37]. What we study is how observables relax to the infinite-time averages following a random fluctuation that can occur at a random time after equilibration.
- [29] By “overwhelmingly” we mean that the conditional probability distribution $P(O_{t'+t}|O_{t'})$ is a Gaussian centered at $C(t)O_{t'}$ whose width is proportional to δ/Δ , where Δ is the uncertainty in energy and δ is the level spacing [27]. It is expected that in quenches in large systems, $\Delta \gg \delta$.
- [30] We have subtracted a constant term containing the infinite-time average of O_t from this correlation function before normalization such that the infinite-time average of $C_{\text{Fluc}}(t)$ is zero.
- [31] M. Srednicki, J. Phys. A **29**, L75 (1996).
- [32] We compute $f(E, \omega)$ by considering those off-diagonal matrix elements of observables whose E falls in a narrow window ΔE around the total energy E_{tot} , and by sorting them by the value of ω . ΔE is chosen such that the results are robust against small changes of ΔE (0.1 for $L = 18$ and 15, and 0.2 for $L = 12$).
- [33] R. Kubo, J. Phys. Soc. Jpn. **12**, 570 (1957).
- [34] L. C. Venuti and P. Zanardi, Phys. Rev. E **87**, 012106 (2013).
- [35] M. Rigol and M. Srednicki, Phys. Rev. Lett. **108**, 110601 (2012); K. He and M. Rigol, Phys. Rev. A **87**, 043615 (2013).
- [36] We have studied the thermalization properties of the system in more detail [26] and found that they are qualitatively similar to those in models with short-range interactions [15].
- [37] P. Reimann, Phys. Rev. Lett. **101**, 190403 (2008).
- [38] The results for the final Hamiltonian in quench type (i) are qualitatively similar to those of the final Hamiltonian in quench type (ii), and are not reported here.
- [39] H. Büchler, A. Micheli, and P. Zoller, Nature Phys. **3**, 726 (2007).
- [40] M. Berninger, A. Zenesini, B. Huang, W. Harm, H.-C. Nägerl, F. Ferlaino, R. Grimm, P. S. Julienne, and J. M. Hutson, arXiv:1212.5584 (2012).
- [41] C. Neuenhahn and F. Marquardt, Phys. Rev. E **85**, 060101 (2012).
- [42] For details, see the Supplementary Materials of Ref. [11].
- [43] M. Rigol, A. Muramatsu, and M. Olshanii, Phys. Rev. A **74**, 053616 (2006).
- [44] A. C. Cassidy, C. W. Clark, and M. Rigol, Phys. Rev. Lett. **106**, 140405 (2011).

Supplementary Materials: Fluctuation-Dissipation Theorem in an Isolated System of Quantum Dipolar Bosons after a Quench

Ehsan Khatami¹, Guido Pupillo², Mark Srednicki³, and Marcos Rigol⁴

¹*Department of Physics, University of California, Santa Cruz, California 95064, USA*

²*IPCMS (UMR 7504) and ISIS (UMR 7006), Université de Strasbourg and CNRS, Strasbourg, France*

³*Department of Physics, University of California, Santa Barbara, California 93106, USA*

⁴*Department of Physics, The Pennsylvania State University, University Park, Pennsylvania 16802, USA*

EXPERIMENTAL RELEVANCE OF OUR MODEL

Hamiltonian (1) in the main text provides a microscopic description for the dynamics of a gas of bosonic ground state molecules such as, e.g., LiCs molecules (dipole moment $d_{\max} \approx 5.6$ Debye), confined transversely (longitudinally) by a two-dimensional (one-dimensional) optical lattice with frequency ω_{\perp} (ω_{\parallel}), with $\omega_{\perp} \gg \omega_{\parallel}$. The molecules are polarized in the transverse direction by an external electric field of strength F and are confined to the lowest band of the 1D lattice, provided $\omega_{\parallel} > \max\{V, J, T\}$. Here, $V = d^2/(4\pi\epsilon_0 a_{\parallel}^3)$, with $d \lesssim d_{\max}$ the dipole moment induced by F , a_{\parallel} the lattice spacing in 1D and ϵ_0 the vacuum permittivity. The hard-core condition is obtained by requiring that molecules are trapped with a low-density n , such that the initial system has no doubly occupied sites [39]. The additional condition $n^{-1/2} \gg (d_{\max}^2/\hbar\omega_{\parallel})^{1/3} \simeq 360\text{nm}$ ensures collisional stability [39]. The model in Eq. (1) of the main text can also describe the dynamics of a gas of strongly magnetic atoms such as Dy (dipole moment $d = 10\mu_B$, with μ_B Bohr's magneton) or Er ($d = 7\mu_B$). In this case, the hard-core constraint is achieved by means of magnetic tuning of the short-range scattering length using Feshbach resonances [40], while J/V decreases exponentially with increasing the depth of the 1D lattice [7].

THERMALIZATION

Despite the presence of interactions that have a power-law decay with distance, we find that the behavior of eigenstate expectation values of few-body observables, as well as thermalization properties of the systems described by Hamiltonian (1) of the main text, are qualitatively similar to those already seen in models with short-range (nearest and next-nearest-neighbor) interactions [15, 41].

In order to show that this is indeed the case, here we study the difference between the results of the diagonal ensemble for the few-body observables studied in main text, namely, n_j and n_k , as well as for the density-density structure factor, N_k (not studied in the main text), and the results of the microcanonical ensemble. The momentum distribution function and the

density-density structure factor are defined as

$$\hat{n}_k = \frac{1}{L} \sum_{l,m} e^{ik(l-m)} \hat{b}_l^\dagger \hat{b}_m, \quad \hat{N}_k = \frac{1}{L} \sum_{l,m} e^{ik(l-m)} \hat{n}_l \hat{n}_m. \quad (7)$$

They are the Fourier transforms of the one-particle and density-density correlation matrices, respectively. Since we work at fixed number of particles, $\langle N_{k=0} \rangle = p^2/L$, so we set it to zero without any loss of generality. These observables can be studied in ultracold gases experiments.

We define the microcanonical average for an observable \hat{O} as $O_{\text{micro}} = \frac{1}{\mathcal{N}_{\Delta E}} \sum_{\alpha} O_{\alpha\alpha}$. Here, $\mathcal{N}_{\Delta E}$ is the number of states in the microcanonical window, which is centered around E_{tot} and has a width of ΔE [42]. We average the results over several close values of ΔE for each system size to ensure that they are robust against small changes in ΔE . The values for ΔE are in $[0.2 - 0.25]$ for $L = 12$, and $[0.1 - 0.15]$ for $L = 15$ and 18.

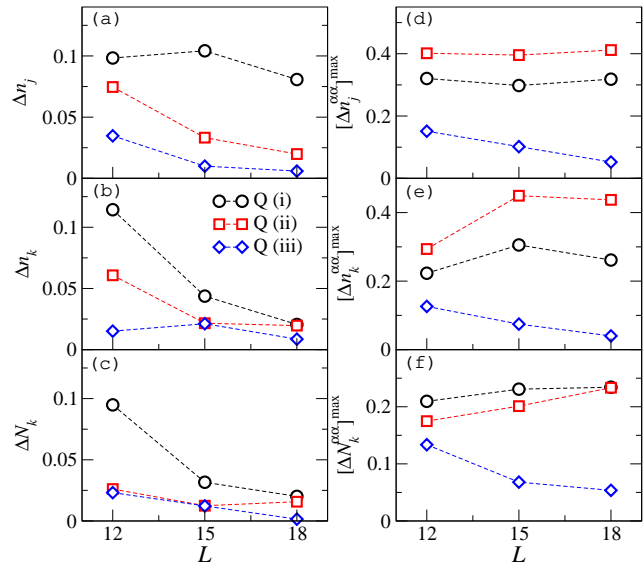


FIG. 4. (a)-(c) Normalized differences between the diagonal and microcanonical ensemble averages for the three observables, n_j , n_k , and N_k [see Eq. (8)] vs L . Different plots in each panel correspond to the three quench types [identified by Q (i), Q (ii), and Q (iii)]. (d)-(f) Maximum of the normalized differences between the microcanonical average and each of the eigenstate expectation values in the microcanonical energy window [see Eq. (9)] vs L .

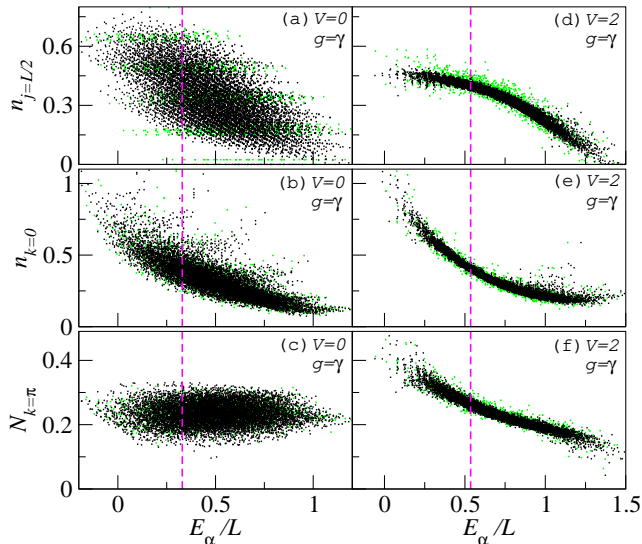


FIG. 5. Eigenstate expectation values values of $\hat{n}_{j=L/2}$, $\hat{n}_{k=0}$, and $\hat{N}_{k=\pi}$ over the entire spectrum vs the scaled eigenenergies for the noninteracting (a)–(c), and interacting system (d)–(f). We show results for $L = 15$ as the green (light colored) points, and for $L = 18$ as the black (dark) ones in each panel. The vertical lines show the location of E_{tot}/L for $L = 18$, which is also roughly equal to that of $L = 15$.

We compute the normalized difference between the predictions of the diagonal and the microcanonical ensembles,

$$\Delta O = \frac{\sum_{\ell} |O_{\text{diag}}(\ell) - O_{\text{micro}}(\ell)|}{\sum_{\ell} O_{\text{diag}}(\ell)}, \quad (8)$$

where ℓ stands for either the site index or the momentum index depending of the observable.

In Fig. 4(a)–(c), we show results for ΔO vs L for the three types of quenches described in the main text. We find that for quench type (i) (between two integrable systems), ΔO is generally larger in comparison to ΔO for the other two quenches, and that this feature remains apparent as the system size increases to $L = 18$. Previous studies, involving the same integrable model without [13, 43, 44] and with [43] the trapping potential and much larger system sizes, have found strong indications that ΔO (where O was either the density or the momentum distribution function) remains finite in the thermodynamic limit so that the system does not thermalize. On the other hand, trends for quench type (iii) suggest that the differences vanish by increasing the system size, i.e., that the nonintegrable dipolar system thermalizes in the thermodynamic limit. The trend is less clear for quench type (ii) as we see that Δn_j monotonically decreases by increasing L , whereas Δn_k and ΔN_k appear to saturate by increasing L from $L = 15$ to $L = 18$. Clearly, larger system sizes are required to confirm whether thermalization takes place for such an integrable system after a quench from a nonintegrable one as argued in Ref. [35].

As mentioned in the main text, for a generic (nonintegrable) system, thermalization can be understood through the ETH.

Here, we examine the validity of the ETH for each case considered by calculating the normalized differences between the observable in each eigenstate and the microcanonical average,

$$\Delta O_{\alpha\alpha} = \frac{\sum_l |O_{\alpha\alpha}(l) - O_{\text{micro}}(l)|}{\sum_l O_{\text{micro}}(l)}, \quad (9)$$

and taking the maximal difference within the microcanonical window, $[\Delta O_{\alpha\alpha}]^{\text{max}} = \text{Max}[\Delta O_{\alpha\alpha}]_{\Delta E}$. This is a measure of how widely the eigenstate expectation values are spread in the microcanonical window. In Fig. 4(d)–4(f), we show this quantity for our three observables vs L . They are seen to consistently decrease with increasing system size for the final Hamiltonian in quench type (iii) while they are seen to saturate to relatively large values for the final Hamiltonians in quenches type (i) and type (ii). This is an indication that eigenstate thermalization occurs in the former case while it fails in the latter ones.

The validity, or failure, of ETH can be perhaps more easily seen by plotting the eigenstate expectation value of observables vs the eigenenergies, as shown in Fig. 5. For the integrable system with $V = 0$ [Fig. 5(a)–5(c)], eigenstate expectation values exhibit large fluctuations inside the microcanonical energy window for both $L = 15$ and 18, and the width of the region where the values are scattered around E_{tot} does not decrease with increasing the system size, i.e., eigenstate thermalization does not occur. This is different from what happens in the nonintegrable case [Fig. 5(d)–5(f)], where each of the eigenstate expectation values of an observable inside a narrow energy window around E_{tot} approaches the microcanonical average as the system size is increased. This is apparent as the width of the region where the values reside around E_{tot} decreases with increasing system size, and presumably vanishes in the thermodynamic limit.

ENERGY SCALES

The short-time evolution of the correlation functions is set by the width of $f(E, \omega)$ as a function of ω , which we denote as W . Note that, as discussed in the main text, f is not well defined for integrable systems and, even for the nonintegrable case for which Eq. (3) of the main text is seen to better describe the data as the system size increases, one cannot disentangle f from the random function $R_{\alpha\beta}$ with merely the knowledge of the off-diagonal values. Therefore, we estimate W for another closely related function, $f_{\text{cg}}(\omega)$, which is obtained by coarse-graining the off-diagonal values. We then calculate the width using

$$W = \frac{2 \int_0^{\infty} |f_{\text{cg}}(\omega)|^2 d\omega}{|f_{\text{cg}}(0)|^2}. \quad (10)$$

Examples of $f_{\text{cg}}(\omega)$ are depicted as lines in the right panels of Fig. 7. We choose different bin sizes for different systems. They are, $50 \times \delta$ for $L = 12$, $300 \times \delta$ for $L = 15$, and $700 \times \delta$ for $L = 18$, where δ is the average level spacing.

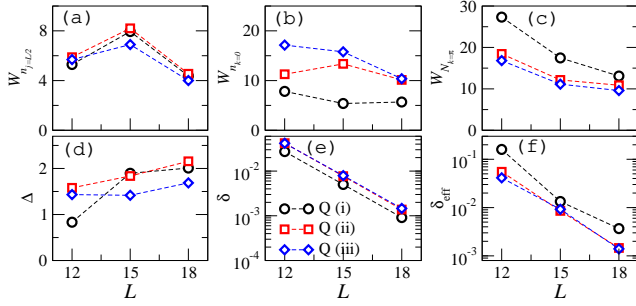


FIG. 6. Various energy scales in the model vs L . Top panels show the estimates for the width of the off-diagonal function, $f(E, \omega)$ in the ω space. (d) shows the uncertainty in the total energy, and (e)-(f) show the average level spacings (see text).

In Fig. 6(a)-6(c), we plot W versus L in the three quenches and for the three observables considered. For $n_{j=L/2}$ and $n_{k=0}$, W varies non-monotonically with L in most cases, while for $N_{k=\pi}$, it is seen to monotonically decrease with increasing L and possibly saturate to a finite value for larger system sizes. Larger system sizes are needed to understand the behavior of W in macroscopic systems. Regardless, the values obtained here can be used in each case to estimate the time scale for the initial decrease of the fluctuation or dissipation correlation functions.

In Fig. 6(d), we also show the quantum uncertainty of the energy, Δ . We find that they are $\mathcal{O}(10^0)$ for the systems studied here, and increase slowly with system size, as expected from the analysis in Ref. [11].

The time scale for recurrences in the correlation functions is set by the average level spacing, δ (estimated by $e^{S(E)}E$ [27]), which, as expected, is found to decrease exponentially with increasing the system size from $\mathcal{O}(10^{-1})$ for $L = 12$ to $\mathcal{O}(10^{-3})$ for $L = 18$ [see Fig. 6(e)]. Therefore, such a time scale for typical system sizes explored in experiments would be much too large to have any relevance. This is also true if one calculates $\delta_{\text{eff}} (= \frac{\Delta}{\sum_{\alpha} |c_{\alpha}|^4})$ [27], shown in Fig. 6(f), which represents the effective level spacing between the eigenstates participating in the diagonal ensemble.

OTHER OBSERVABLES AND/OR SYSTEM SIZE

In the main text, we show the fluctuation and dissipation correlation functions of $n_{j=L/2}$ for the two largest system sizes, $L = 15$ and 18 . For completeness, in Fig. 7, we show the same quantities, as well as the corresponding off-diagonal elements of the two observables shown in Fig. 3 of the main text, for the smallest system we have studied, $L = 12$. Because of the smaller size of the Hilbert space in comparison to the other clusters, some of the trends seen in Fig. 1 of the main text are not so clear in the case of $L = 12$. However, the suppression in the fluctuations of the correlation functions for the nonintegrable case [Fig. 7(c)] is apparent in the corresponding histogram. Other features, such as the dramatic change

in the behavior of the off-diagonal elements of $n_{j=L/2}$ when the integrability-breaking interaction is introduced, is already seen in Figs. 7(d)-7(f) for this small cluster.

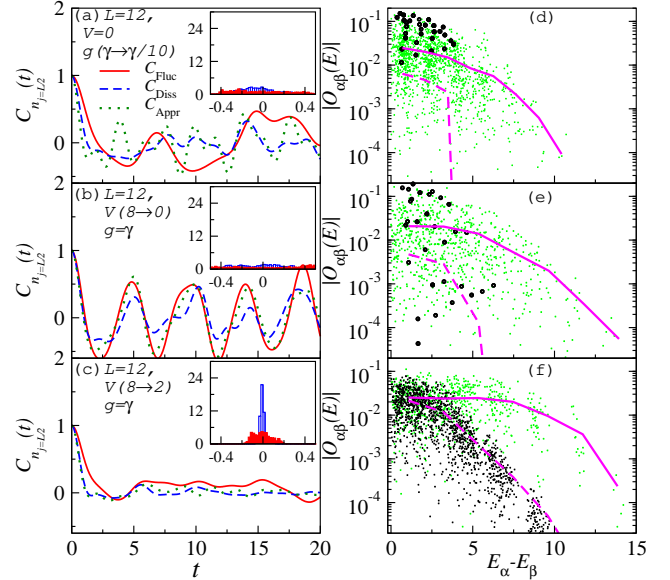


FIG. 7. Left panels (Right panels): the same as Fig. 1 (Fig. 3) of the main text, except that $L = 12$, and that the lines in the right panels are coarse-grained functions of the off-diagonal values used to calculate the width of data in ω using Eq. (10). In the right panels, solid (dashed) lines correspond to $n_{k=0}$ ($n_{j=L/2}$). The bin size for coarse-graining is $50 \times \delta$ for this system size.

In Fig. 8, we show the histograms of the differences between $C_{\text{Fluc}}(t)$ and $C_{\text{Diss}}(t)$, and between $C_{\text{Fluc}}(t)$ and $C_{\text{Appr}}(t)$ for the three quench types studied in the main text and for the two largest system sizes accessible to us. The results in this figure complement those of the normalized variances presented in Fig. 2 of the main text. Figures 8(a) and 8(b) show that, in quenches type (i), there are no signatures of a reduction with increasing system size of the large differences seen between the different correlation functions at each given time (Fig. 1 of the main text). A similar conclusion stands for the behavior of $C_{\text{Fluc}}(t) - C_{\text{Appr}}(t)$ in quenches type (ii) [Fig. 8(d)]. On the other hand, the histograms of $C_{\text{Fluc}}(t) - C_{\text{Diss}}(t)$ in quenches type (ii) [Fig. 8(c)], and of $C_{\text{Fluc}}(t) - C_{\text{Diss}}(t)$ as well as $C_{\text{Fluc}}(t) - C_{\text{Appr}}(t)$ in quenches type (iii) [Fig. 8(e) and 8(f), respectively] make apparent that not only does the variances decrease with increasing system size as shown in Fig. 1 of the main text, but also the maximal differences between the correlation functions at each given time decrease with increasing system size.

In Figs. 9 and 10, we show results for the fluctuation and dissipation correlation functions of $n_{k=0}$ and $N_{k=\pi}$ for the three system sizes and quench types considered in the main text. The contrast between the results for different quenches can be seen to be similar to the one in Fig. 1 of the main text for $n_{j=L/2}$. The main difference between the results for $n_{k=0}$ and $N_{k=\pi}$ when compared to those for $n_{j=L/2}$ is that the former two exhibit smaller fluctuations with increasing system

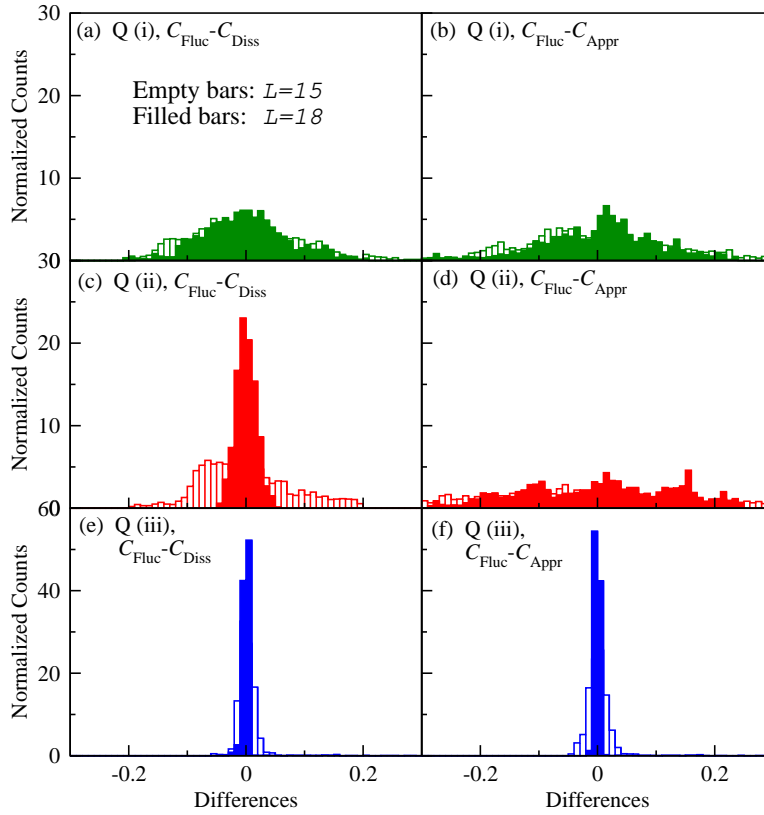


FIG. 8. Normalized histograms of $C_{\text{Fluc}}(t) - C_{\text{Diss}}(t)$ (left panels) and $C_{\text{Fluc}}(t) - C_{\text{Appr}}(t)$ (right panels) for $n_{j=L/2}$, and for the three quenches (from top to bottom) and the two largest system sizes, calculated for 2000 data points between $t = 0$ and 100.

size than the latter one. This is to be expected as the presence of the harmonic trap, which breaks translational symmetry, produces a larger number of nonzero off-diagonal matrix elements of $n_{k=0}$ and $N_{k=\pi}$ in the integrable regime than of $n_{j=L/2}$ (see Fig. 3 of the main text). Still, those fluctuations [see the histograms in the insets of Figs. 9(a)–9(f) and Figs. 10(a)–10(f)] can be seen to be much stronger than in the nonintegrable case [see the histograms in the insets in Figs. 9(g)–9(i) and Figs. 10(g)–10(i)].

The results for the scaling of the variances between

$C_{\text{Fluc}}(t) - C_{\text{Diss}}(t)$ and $C_{\text{Fluc}}(t) - C_{\text{Appr}}(t)$ for $n_{k=0}$ and $N_{k=\pi}$ are presented in Fig. 11. They are also consistent with the conclusions extracted from the scaling of those differences for $n_{j=L/2}$.

Finally, in Fig. 12, we show results for the off-diagonal matrix elements of $N_{k=\pi}$ within ΔE of E_{tot} . Those results are the equivalent of the ones presented in Fig. 3 of the main text for $n_{j=L/2}$ and $n_{k=0}$. That figure shows that the conclusions drawn for the latter two observables in the main text are also applicable to $N_{k=\pi}$.

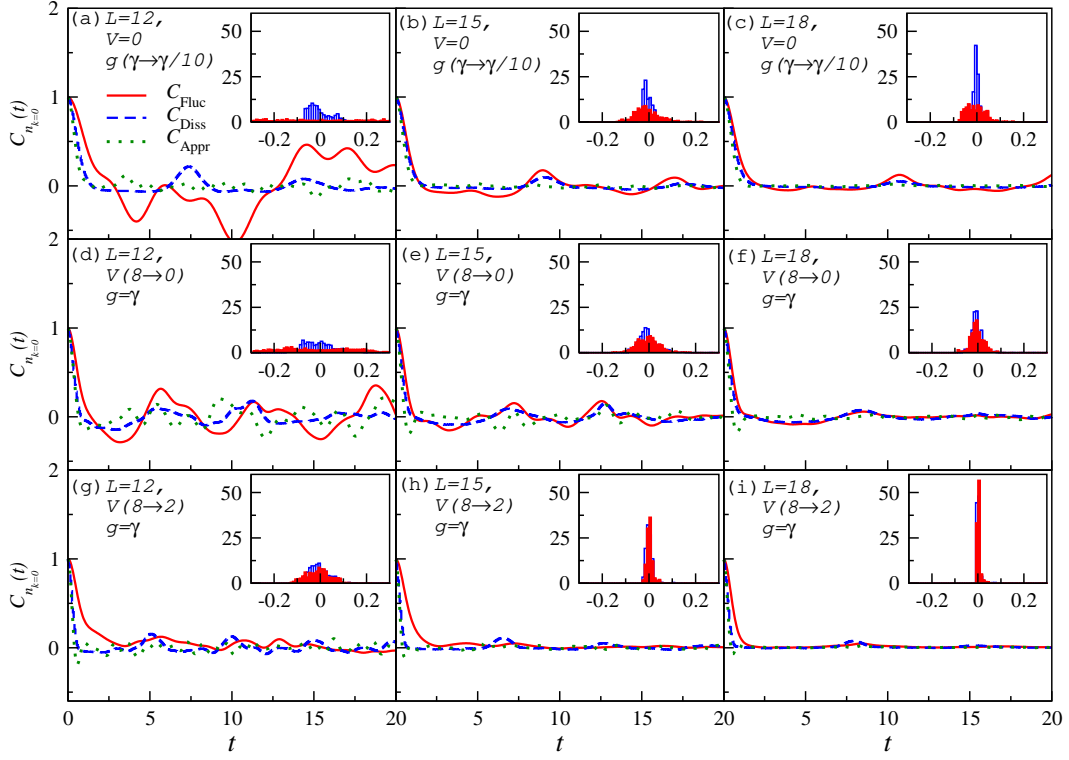


FIG. 9. The same as Fig. 1 of the main text, except that here, the observable is the zero-momentum occupation number, $n_{k=0}$. We have also included the results for $L = 12$ in the left panels.

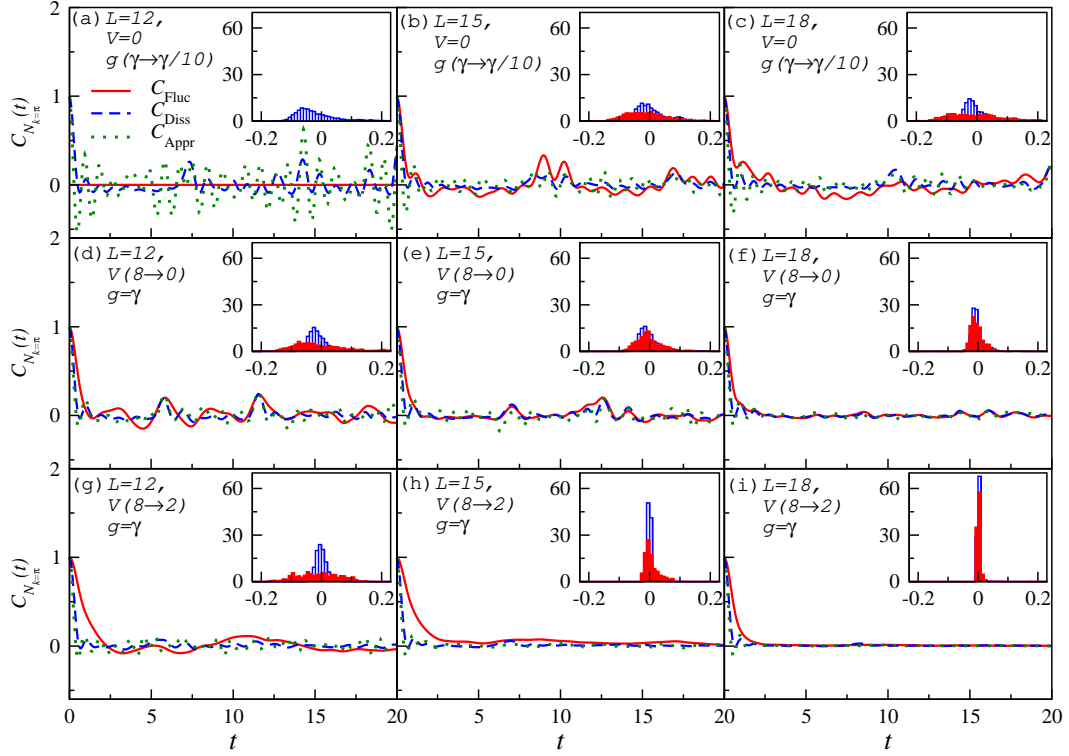


FIG. 10. The same as Fig. 1 of the main text, except that here, the observable is the $k = \pi$ density-density structure factor, $N_{k=\pi}$. We have also included the results for $L = 12$ in the left panels. For quench type (i), we find that the value of $N_{k=\pi}$ for $L = 12$ does not exhibit any dynamics. This is reflected in the corresponding fluctuation correlation function in (a), which is zero at all times. For this reason, we have set $C_{\text{Fluc}}(t) = 0$ in that case and are not showing its histogram. This is unique to $N_{k=\pi}$ for $L = 12$ and to the specific parameters chosen for quench type (i).

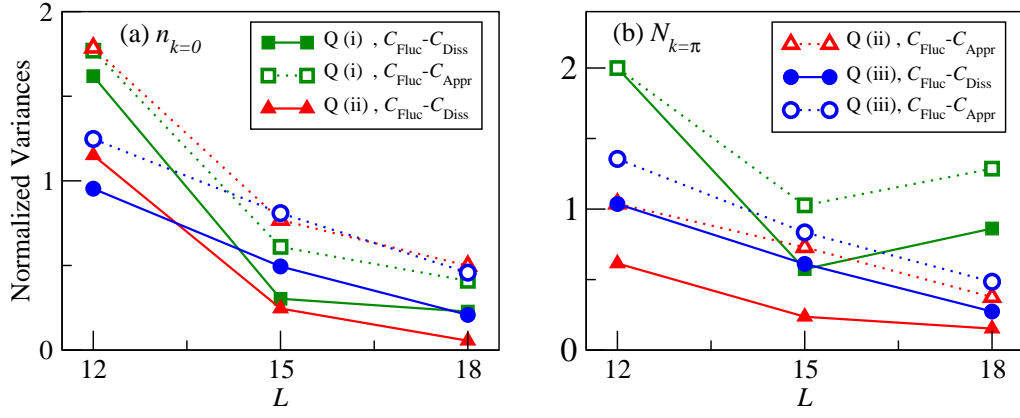


FIG. 11. Same as Fig. 2 of the main text, but for when the observables are $n_{k=0}$ (a), and $N_{k=\pi}$ (b).

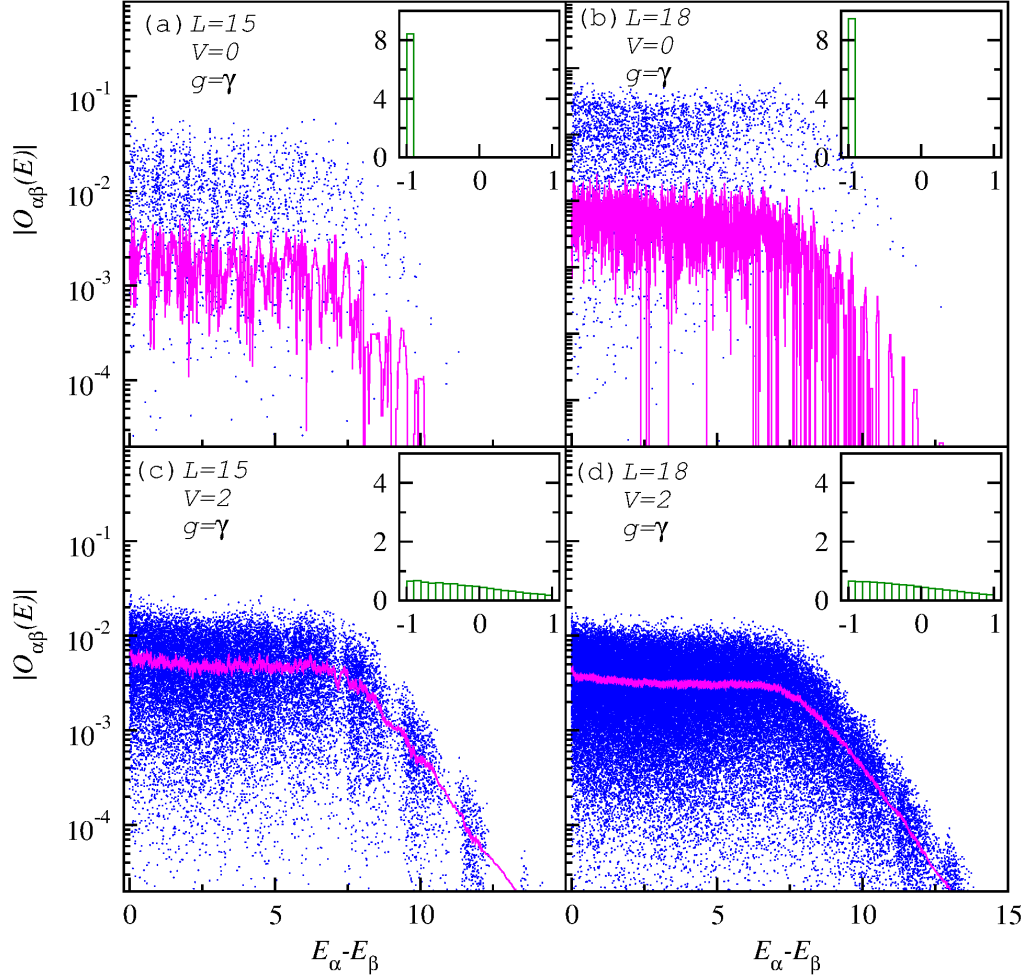


FIG. 12. Same as Fig. 3 of the main text, but for when the observable is $N_{k=\pi}$. Here, we show all the data points in all of the cases. Lines are running averages with a subset length of 100 for $L = 15$ and 1000 for $L = 18$.